Performance of Single-Carrier Block Transmissions Over Multipath Fading Channels With Linear Equalization

Shuichi Ohno, *Member, IEEE*

***Abstract*—We study uncoded bit-error-rate (BER) performances of single-carrier block transmissions, zero-padded (ZP), and cyclic-prefixed (CP) transmission, when linear equalizers are applied and the BERs are averaged over one block. We show analytically that the BER of ZP transmission with linear equalization degrades as the bandwidth efficiency increases, i.e., there is a tradeoff between BER and bandwidth efficiency in ZP transmission. It is also proven that when minimum mean-squared-error (MMSE) equalization is adopted, ZP transmission outperforms CP transmission and uncoded orthogonal frequency-division multiplexing (OFDM) on the average over random channels. However, the difference between the ZP and the CP transmission becomes smaller as the block size gets larger, since the average BER performance of the ZP transmission degrades, while the average BER performance of CP transmission improves, as a function of the block size. Numerical examples are provided to validate our theoretical findings and to compare the block transmission systems.**

***Index Terms*—Block transmission, linear equalization, multipath channel, orthogonal frequency-division multiplexing (OFDM).**

I. Introduction

SEVERE multipath channels often arise in high-rate digital transmissions, which necessitates sophisticated equalization at the receiver. Maximum-likelihood (ML) equalization collects the available multipath diversity to improve bit-error-rate (BER) performance, but is computationally demanding. On the other hand, linear equalization often exhibits poor performance due to intersymbol interference (ISI) resulting from the multipath. Block transmissions, including orthogonal frequency-division multiplexing (OFDM) adopted by many standards, e.g., IEEE 802.11a [1] and HIPERLAN/2 [2], and in digital audio/video broadcasting, have been introduced and utilized to mitigate ISI.

In block transmissions, symbols are grouped into blocks. Adding sufficient number of redundant symbols to each block removes inter block interference (IBI), making efficient block-by-block processing available. In OFDM, a copy of the tail of a block, which is called *cyclic prefix* (CP) is appended at the top of the block. CP with inverse fast Fourier transform (IFFT) at the transmitter and fast Fourier transform (FFT) at the receiver leads to multicarrier systems, including OFDM. OFDM renders a convolution channel into parallel flat channels, which enables very simple one-tap frequency-domain equalization. However, OFDM suffers from 1) fading in the frequency domain, which necessitates powerful but bandwidth consuming channel coding; 2) intercarrier interference (ICI) due to frequency offset between the transmitter and the receiver; and 3) high peak-to-average power ratio, which makes the OFDM signal very sensitive to nonlinear effects in the power amplifiers of the transmitter or receiver [3].

Most of the drawbacks of OFDM arise from parallel transmission on multiple multicarriers due to IFFT at the transmitter. To avoid these drawbacks, single-carrier CP transmission discards the IFFT at the transmitter. Although there is no IFFT operation at the transmitter, efficient frequency-domain equalization is available at the receiver [4], [5]. In single-carrier CP transmission, the symbols are transmitted on a single carrier so that it enjoys the benefits of single-carrier transmissions as well as block transmissions. Precoded OFDM has also been proposed, e.g., in [6] and [7], where the transmitted block is precoded to enhance the error-rate performance. Indeed, single-carrier CP transmission and OFDM can be considered as special cases of precoded OFDM [8]. It has been shown in [9] and [10] that OFDM has the worst performance among precoded OFDM systems and that single-carrier CP transmission exhibits the best performance.

Zero-padded (ZP) transmission is another class of single-carrier block transmissions [11], where it inserts redundant zeros instead of CP into each transmitted block. Sufficient number of guard zeros separate two consecutive received blocks and eliminate IBI. It also has guaranteed symbol detectability regardless of the zero locations of the underlying finite impulse response (FIR) channel [6]. Guaranteed symbol detectability ensures performance improvement at moderate and high signal-to-noise ratio (SNR) [8], [12] and enables blind unknown channel identification [6]. For ZP transmission with ML equalization or even with zero-forcing (ZF) equalization at high SNR [13], full multipath diversity gain is enabled to enhance the system performance. However, with ML equalization, conventional single-carrier transmissions with guard zeros at the beginning and at the end of the transmission but without zero insertions between blocks also exhibit maximum diversity [14]. Since the bandwidth efficiency of ZP is reduced by redundant zeros inserted between blocks, ZP transmission with ML equalization is inferior to conventional single-carrier transmissions in terms of bandwidth efficiency. In this sense, the benefits of ZP transmission should come from linear processing.

Manuscript received January 11, 2005; revised November 7, 2005. The associate editor coordinating the review of this manuscript and approving it for publication was Prof. John J. Shynk.

The author is with the Department of Artificial Complex Systems Engineering, Hiroshima University, Higashi-Hiroshima 739-8527, Japan (e-mail: o.shuichi@ieee.org).

Digital Object Identifier 10.1109/TSP.2006.879321

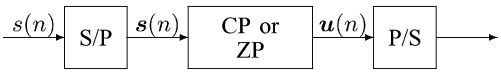

Fig. 1. Part of block transmission at the transmitter.

CP and ZP transmission enable relatively low-complexity block-by-block processing with linear ZF or minimum mean-square-error (MMSE) equalization at the receiver [5], [11]. Although their performances can be demonstrated by numerical simulations, it still remains unclear which is better in BER performance. As the block size gets larger, the performances of CP and ZP transmission converge to conventional single-carrier transmissions. However, the relation between BER performance and bandwidth efficiency has not been fully addressed when a linear equalization is employed. Studying BER performances of CP and ZP transmission analytically, we will answer these fundamental questions.

This paper deals with block transmissions with linear equalization. Our performance measure is the BER averaged over one block. We first show that for every channel, the performance of ZP transmission with ZF or MMSE equalization degrades as its block size increases. There exists a clear tradeoff between BER and bandwidth efficiency. This implies that at low SNR, ZP with long block size cannot take advantage of multipath diversity gain. However, it is also proved that ZP transmission with MMSE equalization outperforms the uncoded OFDM, which justifies the advantage of zero insertions between blocks. We also compare ZP transmission with CP transmission. ZP transmission having a smaller block size by L than CP transmission has better performance than the CP transmission. Unlike ZP transmission, the average BER performance of CP transmission with MMSE equalization improves as the block size is doubled. Based on these facts, we establish that when MMSE equalization is adopted, on the average over random channels, CP transmission is inferior to ZP transmission of the same block size. However, their performance difference converges to zero, as the block size gets larger. Numerical simulations are provided to validate our theoretical findings as well as to compare single-carrier ZP and CP transmission.

II. Block Transmission System and Linear Equalization

We consider point-to-point wireless block transmissions over time-flat but frequency-selective fading channels. A schematic diagram of baseband equivalent block transmissions is depicted in Fig. 1. The information-bearing sequence $\{s(n)\}$ is grouped into blocks $\boldsymbol{s}(n) = [s(Mn+1), \ldots, s(Mn+M)]^T$ of size M. To mitigate the effects of frequency selective channels, we add M_0 redundant symbols to each information block to obtain transmitted blocks $\{\boldsymbol{u}(n)\}$ of size $N := M + M_0$.

There are two major ways to insert redundant symbols: one is to append a copy of the last M_0 information symbols to the top of the information block, which is the CP. At the receiver, the received signals corresponding to the CP are discarded. CP with IFFT at the transmitter and with FFT at the receiver results in OFDM. Since single-carrier CP transmission without IFFT/FFT exhibits better performance than the (uncoded) OFDM and precoded OFDM [6], [7], as shown in [9], [10], we only consider single-carrier CP transmission, which we just call CP transmission in the following. Another insertion of redundant symbols is to pad M_0 zeros at the end of each block to form ZP transmitted blocks, which is known as ZP transmission [11].

Our discrete-time baseband equivalent FIR channel $\{h(l)\}$ has order L and is considered linear time-invariant. At the receiver, we assume perfect timing and carrier synchronization. We collect N noisy samples in an $N \times 1$ received vector. In CP transmission, we remove the M_0 samples which correspond to the CP symbols. If the number M_0 of redundant symbols is greater than or equal to the channel order L, i.e., $M_0 \geq L$, IBI is completely eliminated, and we obtain [11]

$$\boldsymbol{x}(n) = \boldsymbol{H}_M \boldsymbol{s}(n) + \boldsymbol{v}(n) \tag{1}$$

where $\boldsymbol{v}(n)$ is additive white Gaussian noise (AWGN) with variance $\sigma_v^2 \boldsymbol{I}$. In CP transmission, $\boldsymbol{x}(n)$ has M entries and $\boldsymbol{H}_M$ is an $M \times M$ circulant matrix with first column $[h(0), h(1), \ldots, h(L), 0, \ldots, 0]^T$. On the other hand, in ZP transmission, $\boldsymbol{x}(n)$ has N entries and $\boldsymbol{H}_M$ is a tall $N \times M$ (truncated) Toeplitz matrix with first column $[h(0), h(1), \ldots, h(L), 0, \ldots, 0]^T$.

We assume that $M_0 \geq L$ so that the IBI is completely removed and omit the block number n in (1) for notational simplicity. Assuming that perfect knowledge of the channel is available at the receiver, let us first evaluate the symbol mean-square error (MSE) of ZF (or, equivalently, least squares (LS)) and minimum mean-square-error (MMSE) equalization for our simple model given by (1), which have been studied e.g., for CP transmission [9], [10], for multiuser code-division multiple-access (CDMA) systems [15], and for multiple-input multiple-output (MIMO) systems [16].

The output of a ZF equalizer can be expressed as

$$\hat{\boldsymbol{s}} = \boldsymbol{s} + \boldsymbol{H}_M^{\dagger} \boldsymbol{v} \tag{2}$$

where $\boldsymbol{H}_M^{\dagger}$ is the pseudoinverse of $\boldsymbol{H}_M$ defined as $\boldsymbol{H}_M^{\dagger} = (\boldsymbol{H}_M^{\mathcal{H}} \boldsymbol{H}_M)^{-1} \boldsymbol{H}_M^{\mathcal{H}}$ with $(\cdot)^{\mathcal{H}}$ denoting complex conjugate transposition. Since $\boldsymbol{v}$ is white Gaussian with variance $\sigma_v^2 \boldsymbol{I}$, the covariance of the effective noise $\boldsymbol{H}_M^{\dagger} \boldsymbol{v}$ is found to be $\sigma_v^2 (\boldsymbol{H}_M^{\mathcal{H}} \boldsymbol{H}_M)^{-1}$. Let us define the SNR as

$$\gamma = \frac{\sigma_s^2}{\sigma_v^2} \tag{3}$$

where σ_s^2 is the variance of $s(n)$. We also define the mth diagonal entry of $(\gamma \boldsymbol{H}_M^{\mathcal{H}} \boldsymbol{H}_M)^{-1}$ as

$$\lambda_m^{(M)} = \left[\left(\gamma \boldsymbol{H}_M^{\mathcal{H}} \boldsymbol{H}_M \right)^{-1} \right]_{m,m}, \quad \text{for } m = 1, \ldots, M \tag{4}$$

where $[\cdot]_{m,n}$ stands for the (m,n)th entry of a matrix. Then, the received SNR for the mth symbol is expressed as $1/\lambda_m^{(M)}$.

On the other hand, the MMSE equalizer for (1) is found to be [17, ch. 12]

$$\begin{aligned} \boldsymbol{G}_M &:= \sigma_s^2 \boldsymbol{H}_M^{\mathcal{H}} \left(\sigma_s^2 \boldsymbol{H}_M \boldsymbol{H}_M^{\mathcal{H}} + \sigma_v^2 \boldsymbol{I} \right)^{-1} \\ &= \gamma \boldsymbol{H}_M^{\mathcal{H}} \left(\gamma \boldsymbol{H}_M \boldsymbol{H}_M^{\mathcal{H}} + \boldsymbol{I} \right)^{-1}. \end{aligned} \tag{5}$$

The mth entry of the equalized output $\hat{s} = \boldsymbol{G}_M \boldsymbol{x}$ can be expressed as

$$\hat{s}_m = a_m s_m + w_m \tag{6}$$

where a_m is the mth diagonal entry of $\boldsymbol{G}_M \boldsymbol{H}_M$. From (5), we have

$$\begin{aligned} E\{\hat{\boldsymbol{s}}\hat{\boldsymbol{s}}^{\mathcal{H}}\} &= \boldsymbol{G}_M E\{\boldsymbol{x}\boldsymbol{x}^{\mathcal{H}}\}\boldsymbol{G}_M^{\mathcal{H}} \\ &= \sigma_s^4 \boldsymbol{H}_M^{\mathcal{H}} \left(\sigma_s^2 \boldsymbol{H}_M \boldsymbol{H}_M^{\mathcal{H}} + \sigma_v^2 \boldsymbol{I}\right)^{-1} \boldsymbol{H}_M \qquad (7) \\ &= \sigma_s^2 \boldsymbol{G}_M \boldsymbol{H}_M \qquad (8) \end{aligned}$$

where $E\{\cdot\}$ stands for expectation. Since a_m is the mth diagonal entry of $\boldsymbol{G}_M \boldsymbol{H}_M = \sigma_s^2 \boldsymbol{H}_M^{\mathcal{H}} (\sigma_s^2 \boldsymbol{H}_M \boldsymbol{H}_M^{\mathcal{H}} + \sigma_v^2 \boldsymbol{I})^{-1} \boldsymbol{H}_M$, we obtain from (7) that $E\{|\hat{s}_m|^2\} = \sigma_s^2 a_m$. Then, from (6), the noise w_m in (6) is found to have zero mean and variance given by

$$E\left\{|w_m|^2\right\} = E\left\{|\hat{s}_m|^2\right\} - a_m^2 E\left\{|s_m|^2\right\} = \sigma_s^2 a_m (1 - a_m). \tag{9}$$

It follows that the signal-to-interference-noise-ratio (SINR) for the mth symbol is $\sigma_s^2 a_m^2 / [\sigma_s^2 a_m (1 - a_m)] = a_m/(1 - a_m)$.

The (m, m)th entry of $(\gamma \boldsymbol{H}_M^{\mathcal{H}} \boldsymbol{H}_M + \boldsymbol{I})^{-1}$, denoted as $\mu_m^{(M)}$, is related to a_m such that $\mu_m^{(M)} = 1 - a_m$. (See Appendix I for a derivation.) We can therefore re-express the SINR for the mth symbol as

$$\text{SINR}_m := \frac{a_m}{1 - a_m} = \frac{1}{\mu_m^{(M)}} - 1. \tag{10}$$

We note that for MMSE equalization, $\hat{s}_m$ is affected by the other transmitted symbols and hence the noise w_m is not strictly Gaussian. However, the Central Limit Theorem guarantees that as the block size gets larger, the noise becomes Gaussian. Thus, we assume that w_m is Gaussian.

Both the $\lambda_m^{(M)}$ for ZF equalization and the $\mu_m^{(M)}$ for MMSE equalization are the MSE of the mth symbol. The SINR is related to the MSE by SINR $= 1/\text{MSE}$ for ZF equalization and by SINR $= 1/\text{MSE} - 1$ for MMSE equalization as pointed out in [10] and [16].

Let us define a function $f(\cdot)$ in SINR to describe a BER or SER performance for a digital modulation with a finite constellation. For all digital modulation schemes, if a symbol-by-symbol detection is employed, $f(\cdot)$ is in general a monotonically decreasing function in SINR. Using $f(\cdot)$, we will investigate the BER or SER performance averaged over one block defined as

$$\frac{1}{M} \sum_{m=1}^{M} f(\text{SINR}_m). \tag{11}$$

Take, for example, the symbol-by-symbol hard detection of quadrature phase-shift keying (QPSK) signaling. The probability of the bit error for the mth symbol is given by $f(\text{SINR}_m) = Q(\sqrt{\text{SINR}_m})$ [18], where $Q(\cdot)$ is the error function such that $Q(x) = 1/\sqrt{2\pi} \int_x^\infty e^{-t^2/2} dt$. As has been shown, SINR_m is a function of $\lambda_m^{(M)}$ for ZF equalization and $\mu_m^{(M)}$ for MMSE equalization. Thus, all we have to do is to investigate the properties of $\lambda_m^{(M)}$ and $\mu_m^{(M)}$.

III. Performance of ZP Transmission With Linear Equalizers

In this section, we consider ZP transmission. We remark that since ZP transmission has a tall and full column rank matrix $\boldsymbol{H}_M$ except for null channels, $(\boldsymbol{H}_M^{\mathcal{H}} \boldsymbol{H}_M)^{-1}$ always exists, which implies that symbols can be detected for any channel of order up to L except for null channel.

Let us define a square Hermitian Toeplitz matrix $\boldsymbol{R}$ of infinite size such that $[\boldsymbol{R}]_{m,n} = 0$ if $|m - n| > L + 1$. Then, we denote an $M \times M$ matrix having the first M rows and M columns of $\boldsymbol{R}$ as $\boldsymbol{R}_M$. The following property of Toeplitz matrices is a key to our analysis. (See Appendix II for a proof.)

Lemma 1: Let $\nu_m^{(M)}$ be the mth diagonal entry of the inverse of the $M \times M$ matrix $\boldsymbol{R}_M$ Then, for $m = 1, \ldots M$

$$\nu_m^{(M+1)} \geq \nu_m^{(M)} \tag{12}$$

$$\nu_{m+1}^{(M+1)} \geq \nu_m^{(M)}. \tag{13}$$

Using (12) and (13), we show in Appendix III the proof of Lemma 2.

Lemma 2: Let $f(x)$ be an increasing function in x. Then, for $\{\nu_m^{(k)}\}$ satisfying (12) and (13), it holds that

$$\frac{1}{M+1} \sum_{m=1}^{M+1} f\left(\nu_m^{(M+1)}\right) \geq \frac{1}{M} \sum_{m=1}^{M} f\left(\nu_m^{(M)}\right). \tag{14}$$

From the definition, $\lambda_m^{(M)}$ is the (m, m)th entry of the inverse of $\gamma \boldsymbol{H}_M^{\mathcal{H}} \boldsymbol{H}_M$. It is easily verified that $\gamma \boldsymbol{H}_M^{\mathcal{H}} \boldsymbol{H}_M$ is a Hermitian Toeplitz matrix. Thus, $\{\lambda_m^{(M)}\}$ have the same properties as $\{\nu_m^{(M)}\}$. Similarly, $\gamma \boldsymbol{H}_M^{\mathcal{H}} \boldsymbol{H}_M + \boldsymbol{I}$ is also a Hermitian Toeplitz matrix. Since $\mu_m^{(M)}$ is the (m, m)th entry of the inverse of $\gamma \boldsymbol{H}_M^{\mathcal{H}} \boldsymbol{H}_M + \boldsymbol{I}$, $\{\mu_m^{(M)}\}$ exhibit the same properties as $\{\nu_m^{(M)}\}$.

Usually, the BER (or SER) function is a decreasing function in SINR. SINR is a decreasing function in $\lambda_m^{(M)}$ for ZF equalization and in $\mu_m^{(M)}$ for MMSE equalization. Thus, the BER (or SER) function is an increasing function in $\lambda_m^{(M)}$ for ZF equalization and in $\mu_m^{(M)}$ for MMSE equalization. From Lemma 2, we can state our first main result, as follows.

Theorem 1: Suppose ZP transmissions with ZF or MMSE equalization. Let the number of padded zeros be $M_0 \geq L$, where L is the channel order. Then, for every channel realization, the BER of ZP transmission is a non-decreasing function in the information block size M, that is

$$\text{BER}_{\text{zp},1} \leq \text{BER}_{\text{zp},2} \leq \cdots \leq \text{BER}_{\text{zp},\infty} \tag{15}$$

where $\text{BER}_{\text{zp},M}$ is the BER of a ZP transmission of information block size M.

This theorem states a deterministic and universal characteristics of the BER performance of ZP transmission with linear equalization. It should be remarked that no specific modulations are imposed. Theorem 1 holds true for all digital modulations, as long as they can be characterized by a function relating the

SINR with the BER. For a fixed modulation, the performance depends on the block size and degrades as the block size of the information-bearing symbols increases. It makes sense that if the redundancy per transmitted symbol decreases, i.e., as M increases with M_0 fixed, then the performance gets worse. It is also noted that all the results in this paper are developed for uncoded systems. For coded BER, more analyses are required but are beyond the scope of the paper.

The bandwidth efficiency of a block transmission can be defined as

$$\mathcal{E} := \frac{M}{M+M_0}. \tag{16}$$

For a fixed M_0, the bandwidth efficiency improves as the block size M increases, while the performance degrades as proven in Theorem 1. There exists a clear tradeoff between BER performance and bandwidth efficiency. One has to carefully design the block size to obtain the target BER. Theorem 1 also suggests a simple adaptive transmission scheme similar to the adaptive rate control of error correcting codes: if the target BER performance is not attained with a block size, the receiver asks the transmitter to reduce the block size to obtain a better BER, but we will not pursue further here.

The lower limit of BER is $\text{BER}_{\text{zp},1}$, which is realized by ZP with $M = 1$ and is known as the matched filter bound (MFB). The SINR for both ZF and MMSE equalization is $\sum_{l=0}^{L}|h(l)|^2\gamma$. For BPSK or QPSK modulation, the BER can be expressed as $Q((\sum_{l=0}^{L}|h(l)|^2\gamma)^{1/2})$, which is identical with the approximate BER at high SNR of ML equalization with and without zero padding [8], [12], [14]. On the other hand, as M goes to ∞, $\text{BER}_{\text{zp},M}$ converges to $Q([\gamma/\int_0^1|H(e^{j2\pi f})|^{-2}df]^{1/2})$ for ZF equalization and $Q(\sqrt{1/[\gamma\int_0^1|H(e^{j2\pi f})|^{-2}df+1]-1})$ for MMSE equalization. They are found to be equal to the BER of conventional single-carrier transmissions with ZF and with MMSE equalization, having (ideal) infinite length coefficients. We can conclude that ZP transmission always outperforms conventional single-carrier transmissions if both employ linear equalization.

Since Theorem 1 holds true for every channel realization, averaging the BER over the channel probability density function, we establish Theorem 2.

Theorem 2: Consider ZP transmissions with ZF or MMSE equalization as in Theorem 1. Then, the BER of ZP transmission averaged over random channels is a non-decreasing function in the information block size such that

$$\overline{\text{BER}}_{\text{zp},1} \le \overline{\text{BER}}_{\text{zp},2} \le \cdots \le \overline{\text{BER}}_{\text{zp},\infty} \tag{17}$$

where $\overline{\text{BER}}_{\text{zp},M}$ denotes the average BER of a ZP transmission of information block size M.

Suppose, for example, independent and identically distributed (i.i.d.) Rayleigh channels. The average BER of ML equalization is approximated at high SNR by $(G\gamma)^{-(L+1)}$ with G a constant. The constant G can be viewed as a coding gain if the linear channel convolution is considered as coding over complex field [8], [12]. The slope of the BER-SNR curve, $L+1$, is the diversity order, which comes from i.i.d. Rayleigh channels. Although ZP transmission with ZF equalization has the full diversity gain at high SNR [13], Theorem 2 states that its performance gain gets lost as the block size gets larger.

IV. Performance of CP Transmission With Linear Equalizers

ZP transmission exhibits the same performance characteristics both in ZF equalization and MMSE equalization. However, as will be shown below, this does not always hold true for CP transmission. In CP transmission, $\boldsymbol{H}_M$ in (1) is an $M\times M$ circulant matrix, which we denote $\boldsymbol{H}_{\text{cp},M}$.

The circulant matrix $\boldsymbol{H}_{\text{cp},M}$ can be diagonalized by the discrete Fourier transform (DFT) matrix $\boldsymbol{F}$ and its inverse (IDFT) [19, p. 202], such that

$$\boldsymbol{F}\boldsymbol{H}_{\text{cp},M}\boldsymbol{F}^{\mathcal{H}} = \text{diag}\left[H\left(W_M^0\right), H\left(W_M^1\right), \ldots, H\left(W_M^{M-1}\right)\right] \tag{18}$$

where $W_M := \exp(j2\pi/M)$, $[\boldsymbol{F}]_{m,n} = (1/\sqrt{M})W_M^{(m-1)(n-1)}$, and $H(z)$ is the channel transfer function $H(z) := \sum_{n=0}^{L}h_n z^{-n}$. We assume that there is no channel null at the DFT grids, i.e., at W_M^m for $m\in[0,M-1]$, so that the channel matrix $\boldsymbol{H}_{\text{cp},M}$ can be inverted. From (18), one finds that the diagonal entries of $(\gamma\boldsymbol{H}_{\text{cp},M}^{\mathcal{H}}\boldsymbol{H}_{\text{cp},M})^{-1}$ have the same value given by

$$\lambda^{(M)} := \frac{1}{M\gamma}\sum_{m=0}^{M-1}\frac{1}{|H(W_M^m)|^2}. \tag{19}$$

Unlike ZP transmission, CP transmission does not exhibit an ordered BER performance. To see this, suppose a channel realization $h_0, h_1, \ldots, h_L$. The ZF BER performance of the CP transmission of block size $2M$ is a function of $\lambda^{(2M)}$, which can be expressed as

$$\begin{aligned}\lambda^{(2M)} &= \frac{1}{2M\gamma}\sum_{m=0}^{2M-1}\frac{1}{|H(W_{2M}^m)|^2}\\ &= \frac{1}{2}\left[\frac{1}{M\gamma}\sum_{m=0}^{M-1}\frac{1}{|H(W_M^m)|^2}+\frac{1}{M\gamma}\sum_{m=0}^{M-1}\frac{1}{|H(W_{2M}W_M^m)|^2}\right]\\ &= \frac{1}{2}\left[\lambda^{(M)}+\tilde{\lambda}^{(M)}\right]\end{aligned} \tag{20}$$

where $\tilde{\lambda}^{(M)} = (1/M\gamma)\sum_{m=0}^{M-1}(1/|H(W_{2M}W_M^m)|^2)$. Now we utilize a property of Q function [10, Lemma 2] such that $Q(\sqrt{1/y})$ is convex when $y<1/3$ and concave when $y>1/3$. Suppose a channel such that $(1/M)\sum_{m=0}^{M-1}(1/|H(W_M^m)|^2) > (1/M)\sum_{m=0}^{M-1}(1/|H(W_{2M}W_M^m)|^2)$. Then, $\text{BER}_{\text{cp},M} = Q(\sqrt{1/\lambda^{(M)}}) > Q(\sqrt{1/\tilde{\lambda}^{(M)}})$ for any γ. For γ such that $\lambda^{(M)}, \tilde{\lambda}^{(M)} < 1/3$, it follows from the convexity of the Q function that

$$\text{BER}_{\text{cp},2M} \le \frac{1}{2}\left[\text{BER}_{\text{cp},M}+Q\left(\sqrt{1/\tilde{\lambda}^{(M)}}\right)\right] < \text{BER}_{\text{cp},M}.$$

Suppose another channel such that $(1/M)\sum_{m=0}^{M-1}(1/|H(W_M^m)|^2) < (1/M)\sum_{m=0}^{M-1}(1/|H(W_{2M}W_M^m)|^2)$. Then,

$\text{BER}_{\text{cp},M} = Q(\sqrt{1/\lambda^{(M)}}) < Q(\sqrt{1/\tilde{\lambda}^{(M)}})$ for any γ. For γ such that $\lambda^{(M)}$, $\tilde{\lambda}^{(M)} > 1/3$, since the Q function is concave in this region, we obtain

$$\text{BER}_{\text{cp},2M} \geq \frac{1}{2}\left[\text{BER}_{\text{cp},M} + Q\left(\sqrt{1/\tilde{\lambda}^{(M)}}\right)\right] > \text{BER}_{\text{cp},M}.$$

This shows that there are no universal orders in the BER performance of CP transmission with ZF equalization.

Let us compare CP transmission of block size M with ZP transmission of block size $M-L$. Similar to the derivation for the ZF case, even for MMSE equalization, all the the diagonal entries of $(\gamma \boldsymbol{H}_{\text{cp},M}^{\mathcal{H}} \boldsymbol{H}_{\text{cp},M} + \boldsymbol{I})^{-1}$ have the same value given by

$$\mu^{(M)} := \frac{1}{M}\sum_{m=0}^{M-1} \frac{1}{\gamma\left|H\left(W_M^m\right)\right|^2 + 1}. \tag{21}$$

We prove in Appendix IV that for ZF equalization

$$\lambda^{(M)} \geq \lambda_m^{(M-L)}, \quad \text{for all } m \in [1, M-L], \tag{22}$$

and that for MMSE equalization

$$\mu^{(M)} \geq \mu_m^{(M-L)}, \text{ for all } \ m \in [1, M-L] \tag{23}$$

where the equality holds if and only if the channel is a pure delay, that is, $H(z) = cz^{-l}$ for $c \neq 0$. Since the BER function $f(x)$ increases with x, we can conclude Theorem 3.

Theorem 3: Consider CP transmission of block size M and ZP transmission of block size $M-L$. If ZF or MMSE equalization is used, the BER of CP transmission is worse than the BER of ZP transmission, i.e.,

$$\text{BER}_{\text{cp},M} \geq \text{BER}_{\text{zp},M-L} \tag{24}$$

where the equality holds if and only if the channel is a pure delay.

We have evaluated the performance in terms of the SNR γ. For a fixed SNR, $E_s/N_0 = \gamma$ for ZP transmission and $E_s/N_0 = (M+M_0)\gamma/M$ for CP transmission, where E_s denotes the energy per symbol and $N_0 = \sigma_v^2$. If we set the same E_s/N_0 for ZP and CP transmission, the value of γ of CP transmission becomes smaller than the value of γ of ZP transmission. In other words, to keep the same value of γ, additional power in E_s is required for CP transmission. Equation (24) holds true not only in γ but also in E_s/N_0. When comparing the BER for CP and ZP for the same total transmit power per symbol, E_s, the inequality in (24) will only get accentuated further.

Since single-carrier CP transmission with MMSE equalization exhibits better performance than the OFDM [10, Theorem 2], Theorem 3 also leads to Theorem 4.

Theorem 4: For any block size M, ZP transmission with MMSE equalization outperforms the OFDM transmission.

Assuming that the noise in (6) is Gaussian, the BER can be (approximately) evaluated from a linear function of Q functions, which is specific to the underlying modulation scheme. Take, for example, QPSK modulation. Then, the BER is given by $Q(\sqrt{1/\mu^{(M)} - 1})$. Since $\mu^{(M)}$ lies between 0 and 1, $Q(\sqrt{1/\mu^{(M)} - 1})$ is a strictly convex function in $\mu^{(M)}$ [10, Lemma 4]. The convexity for other modulations was also shown in [16].

Since SINR is inversely proportional to $\mu^{(M)}$, we may say that the BER is a concave function of SINR. Similar to (20), one can show that

$$\mu^{(2M)} = \frac{1}{2}\left(\mu^{(M)} + \tilde{\mu}^{(M)}\right) \tag{25}$$

where $\tilde{\mu}^{(M)} = (1/M)\sum_{m=0}^{M-1}(1/(\gamma|H(W_{2M}W_M^m)|^2 + 1))$. It follows from the convexity of the Q function that

$$\text{BER}_{\text{cp},2M} \leq \frac{1}{2}\left[\text{BER}_{\text{cp},M} + Q\left(\sqrt{1/\tilde{\mu}^{(M)} - 1}\right)\right]. \tag{26}$$

Averaging (26) over random channels, we prove Theorem 5 in Appendix V.

Theorem 5: Consider CP transmission with MMSE equalization, where CP meets $M_0 \geq L$. If the BER performance is a concave function in SINR, then the BER of CP transmission averaged over random channels satisfies

$$\overline{\text{BER}}_{\text{cp},2M} \leq \overline{\text{BER}}_{\text{cp},M} \tag{27}$$

where $\overline{\text{BER}}_{\text{cp},M}$ denotes the average BER of a CP transmission of information block size M.

Interestingly, unlike ZP transmission, the BER performance of CP transmission with MMSE equalization improves by doubling the block size. However, it should be noted that this theorem holds true only for non-time-selective channels. If the channel is time selective, the performance may get worse as the block size gets large due to time selectivity.

Averaging (24) over random channels, we obtain

$$\overline{\text{BER}}_{\text{cp},M} > \overline{\text{BER}}_{\text{zp},M-L} \tag{28}$$

since the equality in (24) holds only for pure delay channels. Combining this with Theorem 2 and Theorem 5, we have for $M > L$ that

$$\overline{\text{BER}}_{\text{zp},M} \leq \overline{\text{BER}}_{\text{zp},2M-L} < \overline{\text{BER}}_{\text{cp},2M} \leq \overline{\text{BER}}_{\text{cp},M} \tag{29}$$

which proves Theorem 6.

Theorem 6: Consider ZP and CP transmission with MMSE equalization. Suppose $M \geq L$ and $M_0 \geq L$. If the BER performance can be expressed by a concave function in SINR, then for any block size M, the average BER of ZP transmission is always smaller than the average BER of CP transmission, i.e.,

$$\overline{\text{BER}}_{\text{zp},M} < \overline{\text{BER}}_{\text{cp},M}, \quad \text{for any } M. \tag{30}$$

This theorem gives an answer to our questions: on the average over random channels, ZP transmission outperforms CP transmission. However, at $M = \infty$, $\text{BER}_{\text{cp},\infty} =$

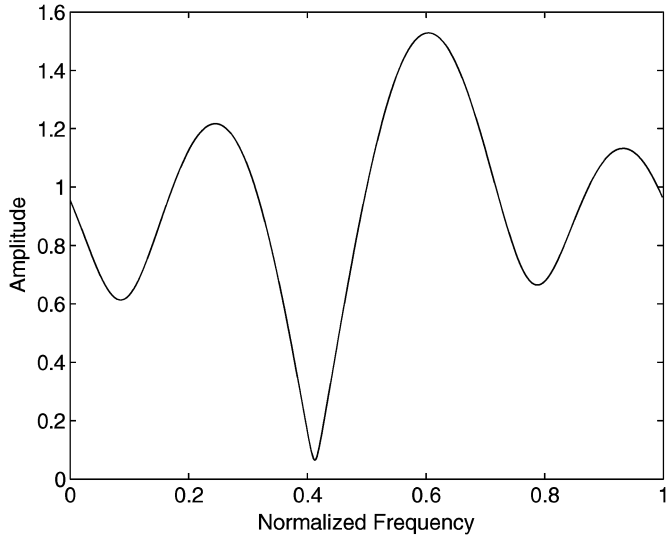

Fig. 2. Magnitude response of the channel, where frequency is normalized by 2π.

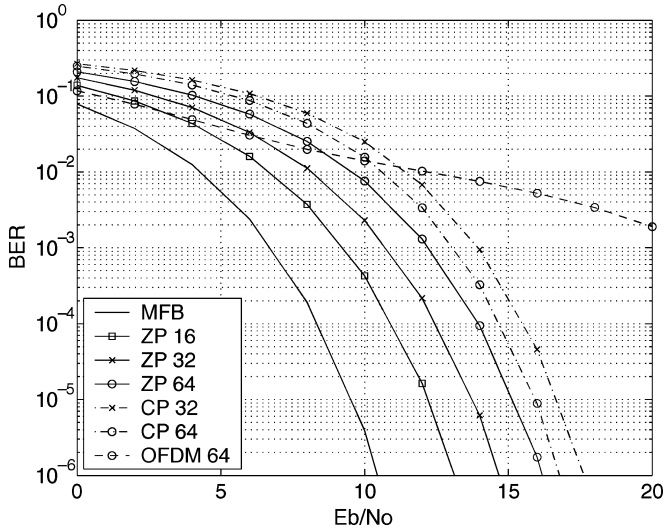

Fig. 3. BER comparison for a fixed channel of order 3 (ZF equalization).

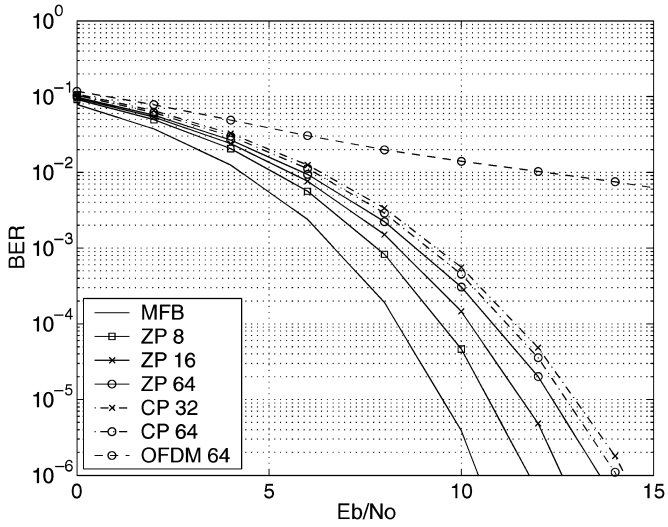

Fig. 4. BER comparison for a fixed channel of order 3 (MMSE equalization).

$\overline{\text{BER}}_{\text{zp},\infty} = Q(\sqrt{1/[\gamma \int_0^1 |H(e^{j2\pi f})|^{-2} df + 1] - 1})$ and hence $\overline{\text{BER}}_{\text{cp},\infty} = \overline{\text{BER}}_{\text{zp},\infty}$. Thus, as the block size gets larger, the performance difference decreases and converges to zero, since $\overline{\text{BER}}_{\text{zp},M}$ increases (cf. Theorem 2), while $\overline{\text{BER}}_{\text{cp},M}$ decreases at least for $M = 2^K$ with integer K (cf. Theorem 5).

V. Numerical Examples

To validate our theoretical findings, we test ZP and CP transmission with ZF and MMSE equalization, abbreviated by ZF-ZP, MMSE-ZP, ZF-CP, and MMSE-CP, with different block sizes for a fixed channel and for random channels, where the number of redundant symbols is set to be eight. The performance of uncoded OFDM with 64 subcarriers is evaluated when hard-decoding was used at their corresponding ZF equalizer outputs. The information symbols are drawn from QPSK constellation.

The fixed channel is of order 3, whose coefficients are [0.5957+0.0101i, -0.3273-0.3472i, -0.2910-0.0533i, 0.1285-0.5599i]. Its amplitude response is illustrated in Fig. 2. Fig. 3 shows BER performance as a function of E_b/N_0. Note that the BER performance of ML is approximately equal to the BER of the ZF-ZP with $M = 1$, i.e., MFB. It is clear from the figure that the performance of ZF-ZP degrades as its information block size increases, which is analytically proved in Theorem 1. ZF-CP does not have such a property. Indeed, ZF-CP of block size 64 has better performance than ZF-CP of block size 32. Remember, however, that this does not always hold true. Even with the same block size, ZF-ZP outperforms ZF-CP, while Theorem 3 assures that ZF-ZP of block size $M - L$ outperforms ZF-CP of block size M. It is also observed that at moderate and high SNR, ZF-ZP has better performance than the uncoded OFDM.

The BER performances of MMSE equalization for the same channel are presented in Fig. 4. Again, we can observe the ordered performance for ZP transmission. However, the performance degradation is not so severe. MMSE-ZP outperforms MMSE-CP but, compared with ZF case, their BER differences are not so large. As suggested by Theorem 4, MMSE-ZP exhibits better performance than the uncoded OFDM for all range of E_b/N_0.

To verify Theorem 2, we generated 10^4 Rayleigh distributed channels of order $L = 7$, having complex zero-mean Gaussian taps with exponential power profile: $E\{|h(l)|^2\} = \exp(-l)/[\sum_l \exp(-l)]$, and averaged the results.

The BER curves are depicted in Fig. 5. At low SNR, OFDM has smaller BER than ZF-ZP and ZF-CP except for $M = 1$. ZF-CP has the worst performance at least till 20 dB. There is no distinguishable difference between ZF-CP with $M = 32$ and with $M = 64$. On the other hand, ZF-ZP gets better than OFDM at high SNR, which is a benefit of the multipath diversity gain. As block size becomes large, however, both BER performances will converge to $Q([\gamma / \int_0^1 |H(e^{j2\pi f})|^{-2} df]^{1/2})$.

ZP and CP transmission with MMSE equalization are compared in Fig. 6. We can verify that as the block size increases, the performance of MMSE-ZP degrades, while the performance

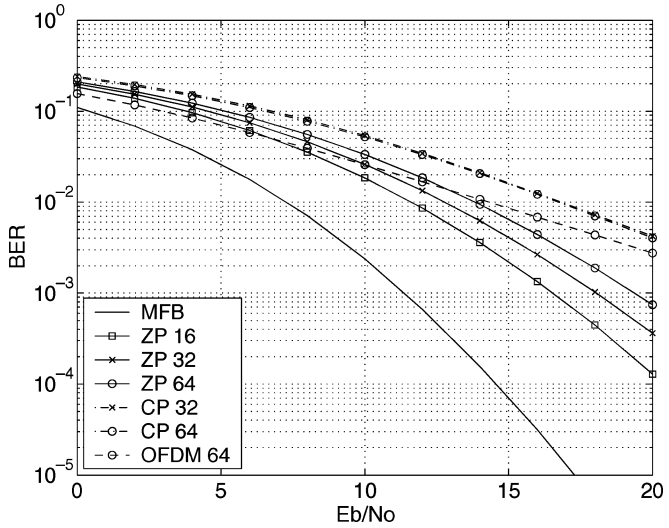

Fig. 5. Average BER comparison for Rayleigh channels of order 7 (ZF equalization).

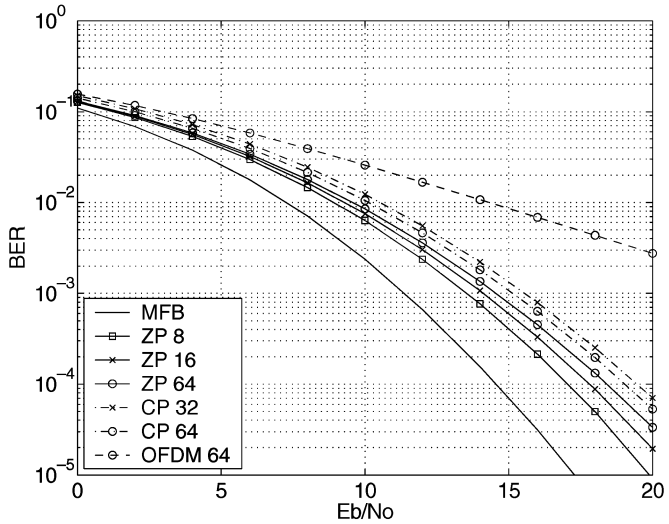

Fig. 6. Average BER comparison for Rayleigh channels of order 7 (MMSE equalization).

of MMSE-CP improves, as suggested by Theorem 2 and by Theorem 5, respectively. Compared with ZF equalization, for moderate block size, there is no significant difference between MMSE-ZP and MMSE-CP, which shows the advantage of MMSE equalization over ZF equalization. Their performance limits, i.e., at M infinity, lie between the BER curves of MMSE-ZP with $M = 64$ and MMSE-CP with $M = 64$.

VI. Conclusion

We have studied two major single-carrier block transmissions, CP and ZP transmission, proposed to mitigate frequency selective multipath propagation. We have shown that when ZF equalization is utilized, the advantage of ZP transmission due to multipath diversity gain is lost as the block size increases. When MMSE equalization is adopted, the BER performance of CP transmission improves as the block size increases, while the BER performance of ZP transmission degrades. We have also proved that on the average over random channels, ZP transmission with MMSE equalization outperforms CP transmission with MMSE equalization and OFDM, which highlights the advantage of ZP transmission with MMSE equalization.

Appendix I
Derivation for $a_m = 1 - \mu_m^{(M)}$

Let us express the singular value decomposition of $\boldsymbol{H}_M^{\mathcal{H}}\boldsymbol{H}_M$ as $\boldsymbol{U}\boldsymbol{\Sigma}\boldsymbol{U}^{\mathcal{H}}$, where $\boldsymbol{U}$ is a unitary matrix and $\boldsymbol{\Sigma}$ is a diagonal matrix. It follows from $(\gamma\boldsymbol{H}_M^{\mathcal{H}}\boldsymbol{H}_M + \boldsymbol{I})^{-1} = (\gamma\boldsymbol{U}\boldsymbol{\Sigma}\boldsymbol{U}^{\mathcal{H}} + \boldsymbol{I})^{-1} = \boldsymbol{U}(\gamma\boldsymbol{\Sigma} + \boldsymbol{I})^{-1}\boldsymbol{U}^{\mathcal{H}}$ that

$$\mu_m^{(M)} = \sum_{n=1}^{M} |u_{mn}|^2 \frac{1}{\gamma[\boldsymbol{\Sigma}]_{n,n} + 1} \tag{31}$$

where u_{mn} is the (m, n)th entry of $\boldsymbol{U}$.

The MMSE estimator is given by $\boldsymbol{G}_M = \gamma\boldsymbol{H}_M^{\mathcal{H}}(\gamma\boldsymbol{H}_M\boldsymbol{H}_M^{\mathcal{H}} + \boldsymbol{I})^{-1}$. From the matrix inversion lemma, we obtain $\gamma\boldsymbol{H}_M^{\mathcal{H}}(\gamma\boldsymbol{H}_M\boldsymbol{H}_M^{\mathcal{H}} + \boldsymbol{I})^{-1}\boldsymbol{H}_M = \gamma(\gamma\boldsymbol{H}_M^{\mathcal{H}}\boldsymbol{H}_M + \boldsymbol{I})^{-1}\boldsymbol{H}_M^{\mathcal{H}}\boldsymbol{H}_M$. Using this, since a_m is the mth diagonal entry of $\boldsymbol{G}_M\boldsymbol{H}_M = \sigma_s^2\boldsymbol{H}_M^{\mathcal{H}}(\sigma_s^2\boldsymbol{H}_M\boldsymbol{H}_M^{\mathcal{H}} + \sigma_v^2\boldsymbol{I})^{-1}\boldsymbol{H}_M = \gamma\boldsymbol{H}_M^{\mathcal{H}}(\gamma\boldsymbol{H}_M\boldsymbol{H}_M^{\mathcal{H}} + \boldsymbol{I})^{-1}\boldsymbol{H}_M = \gamma(\gamma\boldsymbol{H}_M^{\mathcal{H}}\boldsymbol{H}_M + \boldsymbol{I})^{-1}\boldsymbol{H}_M^{\mathcal{H}}\boldsymbol{H}_M = \gamma\boldsymbol{U}(\gamma\boldsymbol{\Sigma} + \boldsymbol{I})^{-1}\boldsymbol{\Sigma}\boldsymbol{U}^{\mathcal{H}}$, we have

$$a_m = \sum_{n=1}^{M} |u_{mn}|^2 \frac{\gamma[\boldsymbol{\Sigma}]_{n,n}}{\gamma[\boldsymbol{\Sigma}]_{n,n} + 1}. \tag{32}$$

Using the identity $\sum_{n=1}^{M} |u_{mn}|^2 = 1$, we finally obtain

$$a_m = \sum_{n=1}^{M} |u_{mn}|^2 \left(1 - \frac{1}{\gamma[\boldsymbol{\Sigma}]_{n,n} + 1}\right) = 1 - \mu_m^{(M)}. \tag{33}$$

Appendix II
Proof of Lemma 1

If $\boldsymbol{R}$ is diagonal, then (12) and (13) follow immediately. Thus, we only consider the case where $\boldsymbol{R}$ is not diagonal.

Since $\boldsymbol{R}_M$ is a Hermitian Toeplitz positive definite matrix, it can be interpreted as the autocorrelation matrix of some stationary process. To prove the lemma, we borrow the results on linear prediction of stationary processes.

Let us consider Yule–Walker equations [20, sec. 3]:

$$\boldsymbol{R}_{M+1}\begin{bmatrix} 1 \\ -\boldsymbol{a}_M \end{bmatrix} = \begin{bmatrix} P_M \\ \boldsymbol{0} \end{bmatrix} \tag{34}$$

where $\boldsymbol{a}_M$ is the predictor vector of size M and P_M is the (forward) prediction error variance.

We partition $\boldsymbol{R}_{M+1}$ as

$$\boldsymbol{R}_{M+1} = \left[\begin{array}{c|c} \boldsymbol{R}_M & \boldsymbol{r}_M^B \\ \hline \boldsymbol{r}_M^{B\mathcal{H}} & r \end{array}\right] = \left[\begin{array}{c|c} r & \boldsymbol{r}_M^{\mathcal{H}} \\ \hline \boldsymbol{r}_M & \boldsymbol{R}_M \end{array}\right] \tag{35}$$

where $\boldsymbol{r}_M^B$ and $\boldsymbol{r}_M$ are $M \times 1$ vectors and $r > 0$. Applying the block matrix inversion lemma to (35), since the forward prediction variance is identical with the backward prediction variance, we obtain

$$\boldsymbol{R}_{M+1}^{-1} = \left[\begin{array}{c|c} \boldsymbol{R}_M^{-1} & \boldsymbol{0} \\ \hline \boldsymbol{0}^T & 0 \end{array}\right] + \frac{1}{P_M}\begin{bmatrix} -\boldsymbol{b}_M \\ 1 \end{bmatrix}\begin{bmatrix} -\boldsymbol{b}_M \\ 1 \end{bmatrix}^{\mathcal{H}} \quad (36)$$

$$= \left[\begin{array}{c|c} 0 & \boldsymbol{0}^T \\ \hline \boldsymbol{0} & \boldsymbol{R}_M^{-1} \end{array}\right] + \frac{1}{P_M}\begin{bmatrix} 1 \\ -\boldsymbol{a}_M \end{bmatrix}\begin{bmatrix} 1 \\ -\boldsymbol{a}_M \end{bmatrix}^{\mathcal{H}} \quad (37)$$

where $\boldsymbol{b}_M = \boldsymbol{R}_M^{-1}\boldsymbol{r}_M^B$ and $\boldsymbol{a}_M = \boldsymbol{R}_M^{-1}\boldsymbol{r}_M$. Comparing diagonal entries of both sides of (36) and (37), we reach to (12) and (13).

Appendix III
Proof of Lemma 2

Let us denote $c_m = f(\nu_m^{(M)})$ and $b_m = f(\nu_m^{(M+1)})$. Then, all we have to prove is

$$M\sum_{m=1}^{M+1} b_m - (M+1)\sum_{m=1}^{M} c_m \geq 0. \quad (38)$$

Since $f(x)$ is an increasing function in x, we have from (12) and (13) that for $m = 1, \ldots, M$

$$b_m \geq c_m, \quad b_{m+1} \geq c_m. \quad (39)$$

For every $k = 1, \ldots, M$, the following equation holds:

$$\sum_{m=1}^{M+1} b_m - \sum_{m=1}^{M} c_m = b_k + \sum_{m=1}^{k-1}(b_m - c_m) + \sum_{m=k+1}^{M+1}(b_m - c_{m-1}). \quad (40)$$

Then, since $b_m - c_m \geq 0$ and $b_m - c_{m-1} \geq 0$ from (39), we have

$$\sum_{m=1}^{M+1} b_m - \sum_{m=1}^{M} c_m \geq b_k \quad \text{for} \quad k = 1, \ldots, M. \quad (41)$$

We can express the left-hand side of (38) as

$$M\sum_{m=1}^{M+1} b_m - (M+1)\sum_{m=1}^{M} c_m = M\left(\sum_{m=1}^{M+1} b_m - \sum_{m=1}^{M} c_m\right) - \sum_{m=1}^{M} c_m. \quad (42)$$

On the other hand, from (41), we obtain

$$M\left(\sum_{m=1}^{M+1} b_m - \sum_{m=1}^{M} c_m\right) = \left(\sum_{m=1}^{M+1} b_m - \sum_{m=1}^{M} c_m\right) + \cdots + \left(\sum_{m=1}^{M+1} b_m - \sum_{m=1}^{M} c_m\right) \quad (43)$$

$$\geq b_1 + b_2 + \cdots + b_M = \sum_{m=1}^{M} b_m. \quad (44)$$

Thus, (42) is lower-bounded such that

$$M\sum_{m=1}^{M+1} b_m - (M+1)\sum_{m=1}^{M} c_m \geq \sum_{m=1}^{M} b_m - \sum_{m=1}^{M} c_m = \sum_{m=1}^{M}(b_m - c_m). \quad (45)$$

It follows again from (39) that

$$M\sum_{m=1}^{M+1} b_m - (M+1)\sum_{m=1}^{M} c_m \geq \sum_{m=1}^{M}(b_m - c_m) \geq 0 \quad (46)$$

which completes the proof of (38).

Appendix IV
Proof of (22) and (23)

For CP transmission with ZF equalization, let us define

$$\boldsymbol{R}_{\mathsf{cp},M} = \gamma \boldsymbol{H}_{\mathsf{cp},M}^{\mathcal{H}} \boldsymbol{H}_{\mathsf{cp},M}. \quad (47)$$

We also define

$$\boldsymbol{R}_{\mathsf{zp},M} = \gamma \boldsymbol{H}_{\mathsf{zp},M}^{\mathcal{H}} \boldsymbol{H}_{\mathsf{zp},M} \quad (48)$$

where $\boldsymbol{H}_{\mathsf{zp},M}$ stands for the channel matrix of ZP transmission of block size M.

It is easy to check that $\boldsymbol{R}_{\mathsf{cp},M}$ can be expressed as

$$\boldsymbol{R}_{\mathsf{cp},M} = \left[\begin{array}{c|c} \boldsymbol{R}_{\mathsf{zp},M-L} & \boldsymbol{C} \\ \hline \boldsymbol{C}^{\mathcal{H}} & \boldsymbol{R}_L \end{array}\right] \quad (49)$$

where $\boldsymbol{R}_L$ is an $L \times L$ matrix and $\boldsymbol{C}$ is an $(M-L) \times L$ matrix. Using the block matrix inversion lemma, we find that

$$\boldsymbol{R}_{\mathsf{cp},M}^{-1} = \left[\begin{array}{c|c} \boldsymbol{R}_{\mathsf{zp},M-L}^{-1} & \boldsymbol{0} \\ \hline \boldsymbol{0} & \boldsymbol{0} \end{array}\right] + \begin{bmatrix} -\boldsymbol{R}_{\mathsf{zp},M-L}^{-1}\boldsymbol{C} \\ \boldsymbol{I}_L \end{bmatrix} \times \boldsymbol{\Delta}^{-1}\begin{bmatrix} -\boldsymbol{R}_{\mathsf{zp},M-L}^{-1}\boldsymbol{C} \\ \boldsymbol{I}_L \end{bmatrix}^{\mathcal{H}} \quad (50)$$

where

$$\boldsymbol{\Delta} = \boldsymbol{R}_L - \boldsymbol{C}^{\mathcal{H}}\boldsymbol{R}_{\mathsf{zp},M}^{-1}\boldsymbol{C}. \quad (51)$$

The matrix $\boldsymbol{\Delta}$ is the Schur complement of $\boldsymbol{R}_{\mathsf{cp},M}$ with respect to $\boldsymbol{R}_{\mathsf{zp},M-L}$. If $\boldsymbol{R}_{\mathsf{zp},M-L}$ is positive definite, then the number of zero eigenvalues of $\boldsymbol{\Delta}$ equals the number of zero eigenvalues of $\boldsymbol{R}_{\mathsf{cp},M}$. Hence, if $\boldsymbol{R}_{\mathsf{cp},M}$ is positive definite then so is $\boldsymbol{\Delta}$.

It follows from (50) and $\boldsymbol{\Delta} > 0$ that at least one diagonal entry of the second term of the right-hand side of (50) is greater than or equal to zero. Noting that all the diagonal entries of $\boldsymbol{R}_{\mathsf{cp},M}^{-1}$ has the same value $\lambda^{(M)}$ and comparing the first $M - L$ diagonal

entries in (50) leads to $\lambda^{(M)} \geq \lambda_m^{(M-L)}$, for all $m \in [1, M-L]$. Since $\boldsymbol{R}_{\mathsf{cp},M}$ is circulant, one finds that $\boldsymbol{C} = 0$ if and only if the channel is a pure delay. Thus, $\lambda^{(M)} = \lambda_m^{(M-L)}$ only when the channel is a pure delay.

When MMSE equalization is used, one can similarly derive $\mu^{(M)} \geq \mu_m^{(M-L)}$ for all $m \in [1, M-L]$, replacing $\boldsymbol{R}_{\mathsf{cp},M}$ with $\boldsymbol{R}_{\mathsf{cp},M} + \boldsymbol{I}$ in (47) and $\boldsymbol{R}_{\mathsf{zp},M}$ with $\boldsymbol{R}_{\mathsf{zp},M} + \boldsymbol{I}$ in (48).

Appendix V

Let us denote the probability density function of a channel with coefficients $\{h_0, h_1, \ldots, h_L\}$ as $p(h_0, h_1, \ldots, h_L)$. Averaging (26) over random channels results in

$$\overline{\mathrm{BER}}_{\mathsf{cp},2M} \leq \frac{1}{2}\left[\overline{\mathrm{BER}}_{\mathsf{cp},M} + \int Q\left(\sqrt{1/\tilde{\mu}^{(M)} - 1}\right) \times p(h_0, h_1, \ldots, h_L) dh_0 dh_1 \cdots dh_L\right] \quad (52)$$

where $\overline{\mathrm{BER}}_{\mathsf{cp},2M}$ is the average BER of CP transmission with MMSE equalization and

$$\overline{\mathrm{BER}}_{\mathsf{cp},M} = \int Q\left(\sqrt{1/\mu^{(M)} - 1}\right) \times p(h_0, h_1, \ldots, h_L) dh_0 dh_1 \cdots dh_L \quad (53)$$

with $\mu^{(M)} = (1/M)\sum_{m=0}^{M-1}(1/(\gamma|H(W_M^m)|^2 + 1))$.

We notice that

$$H\left(W_{2M} W_M^m\right) = \sum_{n=0}^{L} h_n \left(W_{2M} W_M^m\right)^{-n} = \sum_{n=0}^{L} \left(h_n W_{2M}^{-n}\right) W_M^{-mn} \quad (54)$$

and change variables such that

$$\tilde{h}_l = W_{2M}^{-l} h_l, \quad (55)$$

for $l \in [0, L]$. Then, $\tilde{\mu}^{(M)}$ can be expressed as

$$\tilde{\mu}^{(M)} = \frac{1}{M}\sum_{m=0}^{M-1} \frac{1}{\gamma\left|H\left(W_{2M} W_M^m\right)\right|^2 + 1} = \frac{1}{M}\sum_{m=0}^{M-1} \frac{1}{\gamma\left|\sum_{n=0}^{L} \tilde{h}_n W_M^{-mn}\right| + 1}. \quad (56)$$

The Jacobian of the transformation (55) is found to be $W_{2M}^{-1} W_{2M}^{-2} \cdots W_{2M}^{-L}$ so that the probability density function of $\{\tilde{h}_l\}$ can be expressed as

$$p(\tilde{h}_0, \tilde{h}_1, \ldots, \tilde{h}_L) = \frac{p(h_0, h_1, \ldots, h_L)}{W_{2M}^{-1} W_{2M}^{-2} \cdots W_{2M}^{-L}}. \quad (57)$$

Thus, we obtain

$$\int Q\left(\sqrt{1/\tilde{\mu}^{(M)} - 1}\right) p(h_0, h_1, \ldots, h_L) dh_0 dh_1 \cdots dh_L \quad (58)$$

$$= \int Q\left(\sqrt{1/\tilde{\mu}^{(M)} - 1}\right) \times p(\tilde{h}_0, \tilde{h}_1, \ldots, \tilde{h}_L) d\tilde{h}_0 d\tilde{h}_1 \cdots d\tilde{h}_L. \quad (59)$$

This is identical with $\overline{\mathrm{BER}}_{\mathsf{cp},M}$ given by (53). Thus

$$\overline{\mathrm{BER}}_{\mathsf{cp},2M} \leq \frac{1}{2}[\overline{\mathrm{BER}}_{\mathsf{cp},M} + \overline{\mathrm{BER}}_{\mathsf{cp},M}] = \overline{\mathrm{BER}}_{\mathsf{cp},M} \quad (60)$$

which completes the proof.

Acknowledgment

The author would like to thank the anonymous reviewers for their valuable comments and suggestions. The author would also like to thank Dr. Y.-P. Lin for her providing a proof of Lemma 2, which is better than the original proof.

References

[1] *IEEE Standard for Wireless LAN Medium Access Control (MAC) and Physical Layer (PHY) Specifications*, IEEE 802.11, Nov. 1997.

[2] *Broadband Radio Access Networks (BRAN); HIPERLAN Type 2 Technical Specification Part 1—Physical Layer*, DTS/BRAN030003-1, ETSI, Oct. 1999.

[3] R. V. Nee and R. Prasad, *OFDM for Wireless Multimedia Communications*. Norwood, MA: Artech House, Jan. 2000.

[4] D. Falconer, S. L. Ariyavisitakul, A. Benyamin-Seeyar, and B. Eidson, "Frequency domain equalization for single-carrier broadband wireless systems," *IEEE Commun. Mag.*, vol. 40, no. 4, pp. 27–36, Apr. 2002.

[5] B. Muquet, Z. Wang, G. B. Giannakis, M. de Courville, and P. Duhamel, "Cyclic prefixed or zero padded multicarrier transmissions?," *IEEE Trans. Commun.*, vol. 50, no. 12, pp. 2136–2148, Dec. 2002.

[6] A. Scaglione, G. B. Giannakis, and S. Barbarossa, "Redundant filterbank precoders and equalizers Parts I & II," *IEEE Trans. Signal Process.*, vol. 47, no. 7, pp. 1988–2022, Jul. 1999.

[7] X.-G. Xia, "Precoded and vector OFDM robust to channel spectral nulls and with reduced cyclic prefix length in single transmit antenna systems," *IEEE Trans. Commun.*, vol. 49, no. 8, pp. 1363–1374, Aug. 2001.

[8] Z. Wang and G. B. Giannakis, "Complex-field coding for OFDM over fading wireless channels," *IEEE Trans. Inf. Theory*, vol. 49, no. 3, pp. 707–720, Mar. 2003.

[9] Y.-P. Lin and S.-M. Phoong, "BER optimized channel independent precoder for OFDM system," in *Proc. IEEE GLOBECOM*, 2002, pp. 350–354.

[10] ——, "BER minimized OFDM systems with channel independent precoders," *IEEE Trans. Signal Process.*, vol. 51, no. 9, pp. 2369–2380, Sep. 2003.

[11] Z. Wang and G. B. Giannakis, "Wireless multicarrier communications: Where Fourier meets Shannon," *IEEE Signal Process. Mag.*, vol. 47, no. 3, pp. 29–48, May 2000.

[12] Z. Wang, X. Ma, and G. B. Giannakis, "Optimality of single-carrier zero-padded block transmissions," in *Proc. Wireless Communications Networking Conf.*, Orlando, FL, Mar. 17–21, 2002, vol. 2, pp. 660–664.

[13] C. Tepedelenlioğlu, "Low complexity linear equalizers with maximum multipath diversity for zero-padded transmissions," in *Proc. Int. Conf. Acoustics, Speech, Signal Processing (ICASSP) 2003*, Apr. 2003, vol. IV, pp. 636–639.

[14] G. D. Forney, Jr., "Maximum-likelihood sequence estimation of digital sequences in the presence of intersymbol interference," *IEEE Trans. Inf. Theory*, vol. 18, no. 3, pp. 363–378, May 1972.

[15] A. Klein, G. K. Kaleh, and P. W. Baier, "Zero forcing and minimum mean-square-error equalization for multiuser detection in code-division multiple-access channels," *IEEE Trans. Veh. Technol.*, vol. 45, no. 2, pp. 276–287, May 1996.
[16] D. P. Palomar, J. M. Cioffi, and M. A. Lagunas, "Joint Tx–Rx beamforming design for multicarrier MIMO channels: A unified framework for convex optimization," *IEEE Trans. Signal Process.*, vol. 51, no. 9, pp. 2381–2401, Sep. 2003.
[17] S. M. Kay, *Fundamentals of Statistical Signal Processing*. Englewood Cliffs, NJ: Prentice-Hall, 1993, vol. 1.
[18] J. Proakis, *Digital Communications*, 4th ed. New York: McGraw-Hill, 2001.
[19] G. H. Golub and C. F. van Loan, *Matrix Computations*, 3rd ed. Baltimore, MD: The Johns Hopkins Univ. Press, 1996.
[20] S. Haykin, *Adaptive Filter Theory*, 4th ed. Englewood Cliffs, NJ: Prentice-Hall, 2000.

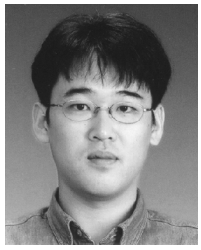

Shuichi Ohno (M'95) received the B.E., M.E., and Dr.Eng. degrees in applied mathematics and physics from Kyoto University, in 1990, 1992, and 1995, respectively.

From 1995 to 1999, he was a Research Associate in the Department of Mathematics and Computer Science at Shimane University, Shimane, Japan, where he became an Assistant Professor. He spent 14 months in 2000 and 2001 at the University of Minnesota as a Visiting Researcher. Since 2002, he has been an Associate Professor with the Department of Artificial Complex Systems Engineering at Hiroshima University, Hiroshima, Japan. His current interests are in the areas of signal processing in communication, wireless communications, and adaptive signal processing.

Dr. Ohno is a member of the IEICE. He served as an Associated Editor for IEEE SIGNAL PROCESSING LETTERS from 2001 to 2003.